JOURNAL OF CATALYSIS **157**, 730–739 (1995)

Ethyl Chloride Decomposition on Oxide-Supported Platinum Catalysts

K. C. McGee, M. D. Driessen, and V. H. Grassian[1]

Department of Chemistry, University of Iowa, Iowa City, Iowa 52242

Received June 1, 1995; revised July 28, 1995

Ethyl chloride decomposition on Pt/SiO_2 and Pt/Al_2O_3 catalysts has been investigated by infrared spectroscopy and mass spectrometry. Ethyl chloride reacts on Pt particles at low temperatures near 200 K to form adsorbed C_2 hydrocarbon fragments. By comparison to literature infrared spectra, three species are identified to be adsorbed on the Pt catalysts—ethyl (C_2H_5), ethylene (C_2H_4), and ethylidyne (C_2H_3). The C_2H_x species coexist to a greater extent on the surface of the Pt particles than on single crystal Pt surfaces. The infrared data suggest there are two different reaction pathways that ethyl chloride may undergo on the Pt particles. The first reaction pathway involves α,β-elimination of HCl to give adsorbed ethylene. The second reaction pathway results from C–Cl bond dissociation to give adsorbed ethyl groups and chlorine atoms. Adsorbed ethyl groups dehydrogenate to ethylidyne upon warming. In the presence of hydrogen, C_2 fragments can be hydrogenated to give ethane. The data show that adsorbed ethyl and ethylene hydrogenate much more readily than ethylidyne. At higher temperatures near 473 K, ethyl chloride reacts on Pt/SiO_2 and Pt/Al_2O_3 to yield gas-phase ethylene, ethane, methane, and hydrogen chloride. The reaction rate is enhanced in the presence of hydrogen and there is a greater amount of ethane produced relative to ethylene. Ethyl chloride can react with the oxide support as well at high temperatures. Surface hydroxyl groups on the alumina support react with ethyl chloride to give ethoxy, $AlOCH_2CH_3$, near 473 K, whereas silica hydroxyl groups show no reaction with ethyl chloride up to 573 K. Possible mechanisms for the high-temperature reaction of ethyl chloride on oxide-supported Pt catalysts are discussed. © 1995 Academic Press, Inc.

INTRODUCTION

In recent years, there have been numerous studies related to the decomposition of halogenated hydrocarbons. These studies are motivated by the need for finding efficient means for the decomposition of hazardous compounds. Metal oxides have been used as catalysts and photocatalysts for the decomposition of chlorinated hydrocarbons (1). Some studies have been directed toward using supported metal catalysts for these reactions and it has been recently suggested that supported Pt catalysts could be effective catalysts for the decomposition of chlorinated hydrocarbons (2, 3).

Previously, we have shown that methyl chloride dissociates on Pt/SiO_2 at low temperatures near 200 K to give adsorbed methyl groups (4). Adsorbed methyl groups readily react with hydrogen to form gas-phase methane. At 473 K, in the presence of hydrogen, methyl chloride is quantitatively converted to methane and hydrogen chloride. In this study, we have investigated the reaction chemistry of ethyl chloride adsorbed on Pt/SiO_2 and Pt/Al_2O_3 catalysts in the presence and absence of hydrogen with infrared spectroscopy and mass spectrometry.

White and co-workers have investigated the surface chemistry of ethyl chloride adsorbed on single-crystal Pt surfaces (5, 6). After adsorption at low temperatures on Pt(111), ethyl chloride quantitatively desorbs into the gas phase upon warming. Although ethyl chloride does not thermally react on Pt(111), it does so upon UV excitation. Broadband irradiation results in carbon–chlorine bond dissociation to form adsorbed ethyl groups and chlorine atoms:

$$C_2H_5Cl(a) \xrightarrow{h\nu} C_2H_5(a) + Cl(a). \qquad [1]$$

The reaction of ethyl groups on the surface was monitored by electron energy loss spectroscopy. As the temperature is raised from 100 to 200 K, ethyl fragments dehydrogenate to form di-σ-bonded ethylene:

$$C_2H_5(a) \rightarrow C_2H_4(a) + H(a). \qquad [2]$$

As the sample is warmed to 320 K, di-σ-bonded ethylene further dehydrogenates to yield ethylidyne:

$$C_2H_4(a) \rightarrow C_2H_3(a) + H(a). \qquad [3]$$

Possible reaction mechanisms for the decomposition of ethyl chloride on oxide-supported Pt catalysts and related

---

[1] To whom correspondence should be addressed.

0021-9517/95 $12.00
Copyright © 1995 by Academic Press, Inc.
All rights of reproduction in any form reserved.

studies on single-crystal surfaces are discussed in more detail below.

METHODS

The IR cell used in these studies has been described previously (7) and is a modification of the design reported by Yates *et al.* (8) and Beebe *et al.* (9, 10). The cell consists of a 1-in.-thick, 2.75-in.-diameter, double-sided conflat flange with two CaF_2 viewports. A 1-in. diameter CaF_2 plate with a uniform layer of the sample is placed in a Cu block assembly. The sample temperature can be varied from 90 to 500 K by circulating cooled or heated nitrogen gas through the copper block. The temperature of the sample is measured with a thermocouple wire placed in direct contact with the CaF_2 plate.

The procedure for preparing the oxide-supported platinum catalysts includes two steps: wet impregnation and chemical processing (10). H_2PtCl_6 (Johnson Matthey Electronics), silica (Degussa Aerosil 200), and alumina (Degussa Aluminum Oxide C) are used to prepare Pt/SiO_2, Pt/Al_2O_3, SiO_2, and Al_2O_3 samples. Samples are made by spraying a slurry of platinum salt/oxide or just oxide suspended in acetone onto a CaF_2 plate (Harshaw). In between applications, the slurry is kept homogeneously mixed by placing the solution in an ultrasonic cleaner. The CaF_2 plate is held on an aluminum template maintained at 328–333 K. A fine mist from the atomizer hits the plate and the acetone flash evaporates, producing a uniform layer of metal salt/support. A template is used to mask half of the sample, allowing one side to be coated with the Pt/oxide support (silica or alumina) and the other side with the oxide only. In some experiments, one side was made with either Pt/oxide support or oxide support and the other side was left blank to monitor gas-phase species. Approximately 10 mg is deposited on each half of the CaF_2 plate. Metal loadings on the order of 10–15% are typically used in these experiments.

After the sample is prepared it is mounted inside the IR cell. The IR cell is wrapped in heating tape and baked out at 473 K for 12–24 h under vacuum. Hydrogen reduction of the metal salt is done at 473 K for 15 min followed by evacuation for the same period of time. This process is sequentially repeated for 30, 60, and 120 min. The sample is subsequently oxidized in O_2 at 473 K and a pressure of 1.0 Torr. The sample is then reduced again at 473 K.

The IR cell is attached to the vacuum chamber through a 2-ft stainless-steel bellows hose. The stainless-steel high-vacuum apparatus consists of a 20 liters/s ion pump, two absolute pressure transducers, for accurate pressure measurements in the range 0.001 to 1000 Torr, and an ion gauge. A turbomolecular pump is used to rough-pump the vacuum chamber and to evacuate the gas manifold line used for sample introduction. Following bake-out, the apparatus reaches a base pressure of $<1 \times 10^{-8}$ Torr.

The Pt/SiO_2 and Pt/Al_2O_3 samples are characterized using several methods. Particle size distributions are determined using scanning transmission electron microscopy (TEM). The micrographs are obtained with a Hitachi H-600 electron microscope operated at an acceleration voltage of 100 kV. Particles as small as 1 nm can be detected. For a 15% Pt/SiO_2 sample, the average diameter of the particles is 2 nm. IR spectroscopy of CO is also used to determine if the sample was fully reduced. Upon CO adsorption, after the last reduction of the catalyst, there were no absorption bands in the infrared that could be associated with CO adsorption on oxidized sites; these bands would have frequencies greater than 2100 cm^{-1} (11).

A UTI Detectorr II mass spectrometer is used to measure gas-phase reactants and products as a function of time. Infrared measurements are made using a Galaxy 6021 FT-IR spectrometer (Mattson Instruments) with a narrowband MCT detector. One thousand scans are taken with an instrument resolution of 4 cm^{-1}. Some of the absorbance spectra have been baseline corrected to remove a sloping background. Because of low-frequency absorptions for the oxide support, only the spectral regions from 1300–4000 and 1000–4000 cm^{-1} are shown for Pt/SiO_2 and Pt/Al_2O_3, respectively.

Ethyl chloride (Mattheson 99.9%) is treated with several freeze–pump–thaw cycles prior to use. Hydrogen (Matheson 99.9995%) and oxygen (Air Products 99.6%) are used without further purification.

RESULTS

1. *Identification of Adsorbed C_2 Hydrocarbon Fragments on Pt/SiO_2 and Pt/Al_2O_3*

Before the mechanism of C_2H_5Cl decomposition on oxide-supported Pt catalysts can be determined, it is important to be able to identify adsorbed hydrocarbon intermediates on the surface of the Pt particles. Sheppard and co-workers have investigated the adsorption of C_2H_4 on Pt/SiO_2 and have identified the presence of five different adsorbed C_2 hydrocarbon species with infrared spectroscopy (12–15). It is well established that ethylene partially dehydrogenates near room temperature to form ethylidyne on Pt single-crystal surfaces and supported Pt catalysts. Three intense absorption bands for adsorbed ethylidyne, C_2H_3, occur near 2880, 2795, and 1342 cm^{-1} on Pt/SiO_2 (12). Additional bands near 2940, 1410, and 1128 cm^{-1} have been identified on Pt/Al_2O_3 catalysts (16, 17).

In addition to ethylidyne, there are three forms of adsorbed ethylene, C_2H_4, that have been characterized. One form is denoted as a π-bonded species with two absorptions near 3016 and 1496 cm^{-1} on Pt/SiO_2 (13) and an additional band near 1200 cm^{-1} on Pt/Al_2O_3 (17). There is another

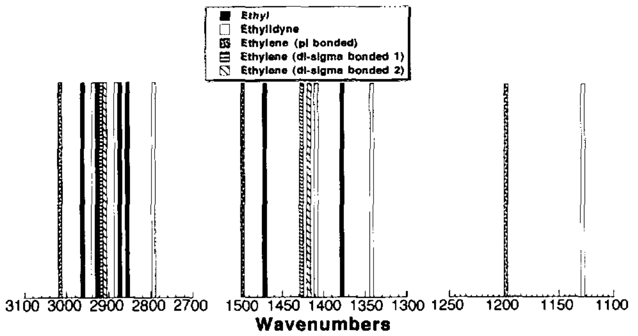

FIG. 1. The absorption band frequencies for five C_2 hydrocarbon fragments: C_2H_5, π-bonded C_2H_4; di-σ-bonded C_2H_4 (1 and 2); and C_2H_3 adsorbed on Pt/SiO_2 and Pt/Al_2O_3 catalysts. See text for further discussion.

form of ethylene denoted as a di-σ-bonded species that has been characterized with infrared spectroscopy. On Pt/SiO_2 it has been postulated that there are two di-σ-bonded species, the difference being the adsorption site. Here, these two forms are denoted as di-σ-bonded 1 and di-σ-bonded 2. Two absorption bands are associated with each of these di-σ-bonded forms of ethylene with frequencies of 2922/1428 and 2906/1419 for di-σ-bonded 1 and di-σ-bonded 2, respectively (14).

C_2H_5 groups have been postulated to form on Pt/SiO_2 and Ni/SiO_2 from the partial hydrogenation of ethylene (15, 18). Absorption bands for adsorbed ethyl groups are near 2960(s), 2930(s), 2875(m), and 2860(w) cm^{-1} in the C–H stretching region and 1470(w) and 1383(w) cm^{-1} in the CH_2/CH_3 deformation region. We have compiled the values of the frequencies of the absorption bands for these five species—ethyl, π-bonded ethylene, di-σ-bonded ethylene (1 and 2), and ethylidyne—in Fig. 1 and use this as a guide in identifying C_2 fragments present on the surface from C_2H_5Cl reaction. The absorption bands are grouped into three spectral regions: 2750–3050 cm^{-1}, corresponding to bands primarily associated with C–H stretching modes; 1300–1500 cm^{-1}, corresponding to bands associated with methyl and methylene bending modes; and 1000–1200 cm^{-1}, corresponding to bands associated with the C–C stretching mode.

2. *Adsorption and Reaction of C_2H_5Cl on Pt/SiO_2 and Pt/Al_2O_3 at Low Temperatures*

We now turn to the infrared spectra recorded after adsorption of C_2H_5Cl on Pt/SiO_2 and Pt/Al_2O_3 near 190 K. Infrared spectra of C_2H_5Cl adsorbed on Pt/Al_2O_3, Al_2O_3, Pt/SiO_2, and SiO_2, in the presence of an equilibrium pressure of gas-phase C_2H_5Cl are shown in Fig. 2. As indicated by the hydroxyl group region near 3600 cm^{-1}, the data clearly show that C_2H_5Cl adsorbs on the oxide support by bonding to the surface hydroxyl groups. For Pt/Al_2O_3 and Al_2O_3 there is a decrease in the integrated area due to free hydroxyl groups at 3730 cm^{-1} concomitant with the growth of a broadband at lower frequency near 3608 cm^{-1}. For Pt/SiO_2 and SiO_2, there is a shift of approximately 166 cm^{-1} to lower frequency of the hydroxyl group frequency upon adsorption of C_2H_5Cl. The shift to lower frequency and increase in bandwidth of the hydroxyl group absorption bands indicate a hydrogen-bonding interaction (19, 20). The spectra obtained for the pure SiO_2 and Al_2O_3 samples are nearly identical to the Pt/SiO_2 and Pt/Al_2O_3 samples except the bands in the Pt/oxide-support spectra are slightly broader. The frequencies of the absorption bands for Pt/oxide support and oxide support are within 4 cm^{-1} of each other. This result can be somewhat expected considering that the surface area of silica and alumina is much greater than that for the Pt particles. The frequencies of the absorption bands for gas-phase C_2H_5Cl (21) and adsorbed C_2H_5Cl, on Pt/Al_2O_3, Al_2O_3, Pt/SiO_2, and SiO_2, are given in Table 1. The frequencies for adsorbed C_2H_5Cl are within 2–14 wavenumbers of the gas-phase values.

The infrared spectra recorded after adsorption and evacuation of 3.5 Torr of C_2H_5Cl on Pt/Al_2O_3 at 190 K as a function of evacuation time are shown in Fig. 3. The absorption bands due to adsorbed C_2H_5Cl decrease significantly upon evacuation at 190 K. C_2H_5Cl desorbs completely from the Al_2O_3 sample after 45 min of evacuation. However, there remains some C_2H_5Cl on the Pt/Al_2O_3 sample after 45 min of evacuation that can be assigned to C_2H_5Cl adsorbed on the Pt particles. The bands near 2971, 2936, 2881, 1440, 1381, 1275, 1237, and 1072 cm^{-1}, assigned to C_2H_5Cl adsorbed on the surface of the platinum parti-

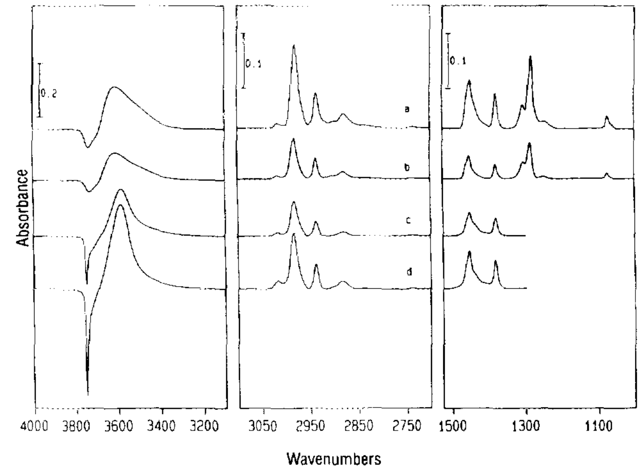

FIG. 2. FT-IR spectra recorded of C_2H_5Cl adsorbed on (a) Pt/Al_2O_3, (b) Al_2O_3, (c) Pt/SiO_2, and (d) SiO_2 near 190 K in the presence of gas phase C_2H_5Cl at an equilibrium pressure of approximately 5 Torr. Contributions from gas-phase absorptions were subtracted from the infrared spectra of adsorbed C_2H_5Cl shown above.

TABLE 1
Vibrational Assignment of Ethyl Chloride Adsorbed on Pt/SiO_2 and Pt/Al_2O_3 in the 950–3100 cm^{-1} Spectral Region

Mode description	Gas phase[a]	Pt/SiO_2[b]	SiO_2[b]	Pt/Al_2O_3[b]	Al_2O_3[b]
			A′		
CH_2 s-stretch	2977	2982	2980	2981	2984
CH_3 d-stretch	2946	2937	2935	2936	2938
CH_3 s-stretch	2881	2884	2883	2881	2884
CH_3 d-deformation	1463	1460(sh)[c]	1460(sh)	1460(sh)	1460(sh)
CH_2 scissor	1448	1452	1452	1449	1452
CH_3 s-deformation	1385	1381	1381	1380	1382
CH_2 wag	1289	n.o.[d]	n.o.	1286	1290
CH_3 rock	1081	n.o.	n.o.	1072	1074
C–C stretch	974	n.o.	n.o.	965	967
			A″		
CH_2 a-stretch	3014	3011	3008	3013	3017
CH_3 d-stretch	2986	2982	2980	2981	2984
CH_3 d-deformation	1448	1452	1452	1449	1452
CH_2 twist	1251	n.o.	n.o.	1237	1249
CH_3 rock	974	n.o.	n.o.	965	967

[a] Ref. (21).
[b] This work.
[c] sh, shoulder.
[d] n.o., not observed due to strong absorptions of the silica support.

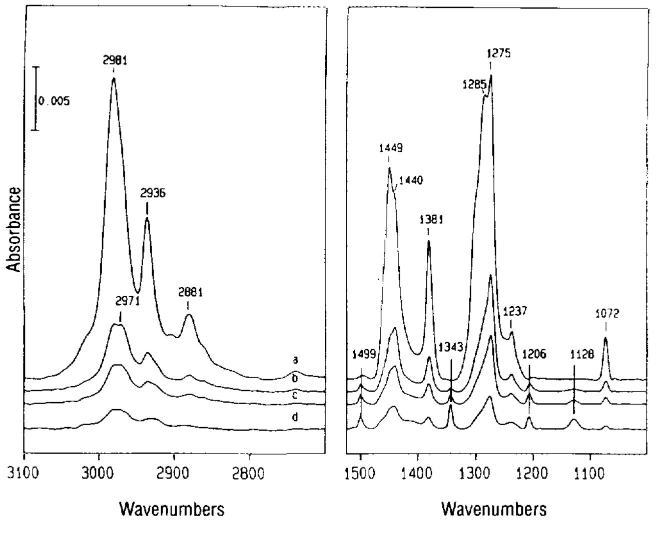

FIG. 3. FT-IR spectra recorded of adsorbed C_2H_5Cl on Pt/Al_2O_3 as a function of evacuation time at 190 K: (a) 5 min, (b) 30 min, (c) 45 min, and (d) 60 min. C_2H_5Cl desorbs from Al_2O_3 after 45 min, but remains on Pt/Al_2O_3 after 60 min of evacuation.

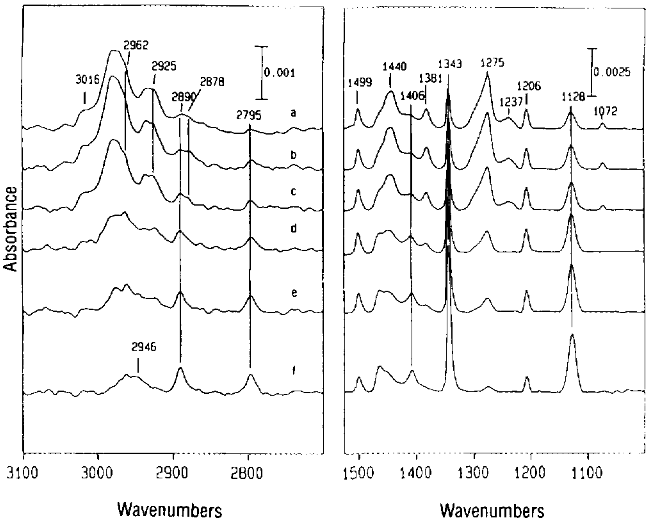

FIG. 4. FT-IR spectra recorded of adsorbed C_2H_5Cl on Pt/Al_2O_3 as a function of temperature: (a) 190 K, (b) 204 K, (c) 222 K, (d) 243 K, (e) 265 K, (f) 289 K.

cles, decrease in intensity as a function of evacuation time and upon warming.

As the bands associated with adsorbed C_2H_5Cl lose intensity, several other bands become apparent in the spectrum. Absorption bands near 3016 (very weak), 1499, and 1206 cm^{-1} can be assigned to π-bonded ethylene (13, 17). These bands begin to grow in after 30 min of evacuation and then level off after 45 min of evacuation. Several other bands present in the spectrum after 60 min of evacuation can be assigned to other C_2 hydrocarbon fragments. The spectrum after 60 min of evacuation is expanded in Fig. 4a. Bands at 2946, 2890, 2795, 1406, 1343, and 1128 cm^{-1}, characteristic of ethylidyne on Pt (12, 16, 17), grow in intensity as the sample is warmed from 190 to 289 K (Fig. 4a–f). According to the metal surface selection rule for a C_{3v} adsorption geometry, the asymmetric modes for ethylidyne at frequencies of 2946 and 1406 should not be observed. However, adherence to this rule is weakened for small metal particles on the order of 2 nm or less (22), which may be the reason why asymmetric modes for adsorbed ethylidyne are observed in this work. As for π-bonded ethylene, the ethylidyne bands are not initially present in the spectrum after evacuation (Fig. 3a), but do grow in as a function of evacuation time (Figs. 3b–d). The ethylidyne bands continue to increase in intensity as the sample is warmed from 190 to 289 K (see Fig. 4), in contrast, the intensity of the bands associated with π-bonded ethylene remain constant as a function of temperature (see Fig. 4).

Another set of bands, not associated with either π-bonded C_2H_4 or ethylidyne, is present after evacuation and most obvious in the spectrum recorded after 60 min of evacuation at 190 K and the spectra recorded between 190

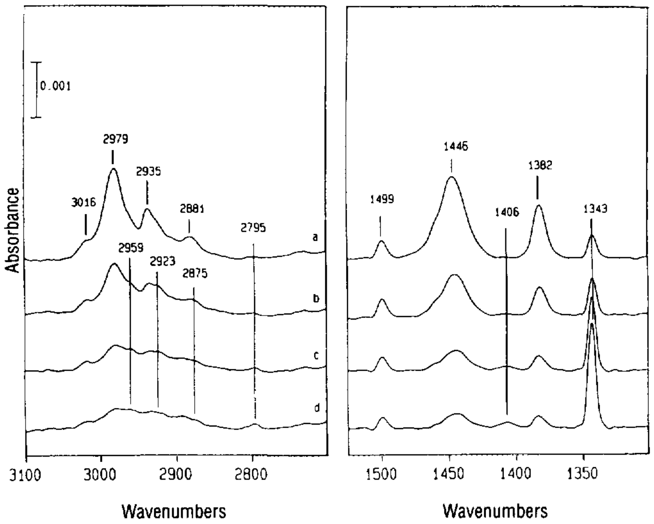

FIG. 5. FT-IR spectra recorded of adsorbed C_2H_5Cl on Pt/SiO_2 as a function of evacuation time at 200 K: (a) 2 min, (b) 15 min, (c) 40 min, and (d) 65 min. C_2H_5Cl desorbs from SiO_2 after 15 min, but remains on Pt/SiO_2 after 65 min of evacuation.

and 243 K. The bands for this other C_2 species appear in the C–H stretching region as shoulders to the parent absorption bands. The frequencies of these new bands near 2962, 2925, and 2878 cm^{-1} match well with the frequencies of the three most intense bands associated with adsorbed ethyl groups on Pt/SiO_2 as observed by de la Cruz and Sheppard from the partial hydrogenation of ethylene (15). Other bands that are expected in the methyl and methylene deformation region for adsorbed ethyl groups are much weaker and have nearly the same frequencies as the bands in this region for the parent molecule C_2H_5Cl. The bands due to adsorbed ethyl groups begin to decrease in intensity as the sample is warmed above 243 K as the bands due to ethylidyne grow (see Fig. 4).

The low-temperature adsorption of ethyl chloride was investigated on a Pt/SiO_2 catalyst as well. The results for ethyl chloride adsorption on Pt/SiO_2 are similar to those discussed above for Pt/Al_2O_3. The spectra for ethyl chloride adsorbed on Pt/SiO_2 near 200 K as a function of evacuation time are shown in Fig. 5. After 5 min of evacuation, ethyl chloride desorbs completely from the pure SiO_2 sample. Bands at 2979, 2935, 2881, 1446, and 1382 cm^{-1} in the spectrum after evacuation are assigned to C_2H_5Cl adsorbed on the Pt particles, in good agreement with the Pt/Al_2O_3 data.

As can be seen in Figs. 5 and 6, C_2H_5Cl adsorbed on Pt/SiO_2 undergoes similar reactions to form π-bonded C_2H_4, ethyl groups, and ethylidyne. At 200 K on Pt/SiO_2, π-bonded ethylene is present upon evacuation of gas-phase C_2H_5Cl and its absorption bands do not grow in intensity as a function of temperature (Fig. 6). Ethylidyne absorption bands increase in intensity upon evacuation (Fig. 5) and as the sample is warmed from 200 to 286 K (Fig. 6). After 15 min. of evacuation the bands at 2959, 2923, and 2872 cm^{-1} become apparent in the spectrum (Figs. 5b–d). Similar to the Pt/Al_2O_3 spectra, these bands are assigned to adsorbed ethyl groups. There is a decrease in intensity of the bands associated with adsorbed C_2H_5Cl and C_2H_5 as the sample is warmed to 286 K. If the sample valve is closed to the pumps during warming, the infrared spectrum shows that some adsorbed C_2H_5Cl desorbs upon warming as indicated by the presence of gas-phase C_2H_5Cl absorption bands. If an infrared spectrum is recorded after the sample warms to near room temperature and is left there for several hours, the spectrum shows only the presence of ethylidyne, indicating that all of the π-bonded ethylene either desorbs or is displaced from the surface at room temperature over time (spectrum not shown).

3. *Reaction of Adsorbed C_2 Fragments with Hydrogen*

The reactivity of C_2 fragments formed from C_2H_5Cl dissociation with hydrogen was monitored with infrared spectroscopy as well. Figure 7a shows the IR spectrum recorded after adsorption of C_2H_5Cl (3.5 Torr) on Pt/SiO_2 at 200 K followed by 15 min of evacuation. The spectrum shows the presence of C_2H_5Cl (2979, 2935, 2881, 1441, and 1381 cm^{-1}), C_2H_5 (2959, 2923, 2872 cm^{-1}), π-bonded C_2H_4 (3016 and 1499 cm^{-1}) and C_2H_3 (1343 cm^{-1}). The spectrum recorded after addition of 0.5 Torr of H_2 into the IR cell for 5 min followed by evacuation is shown in Fig. 7b. Most evident is the disappearance of absorption bands due to ethyl groups and π-bonded ethylene, which reacts to form gas-phase ethane. In contrast, the ethylidyne and ethyl chloride

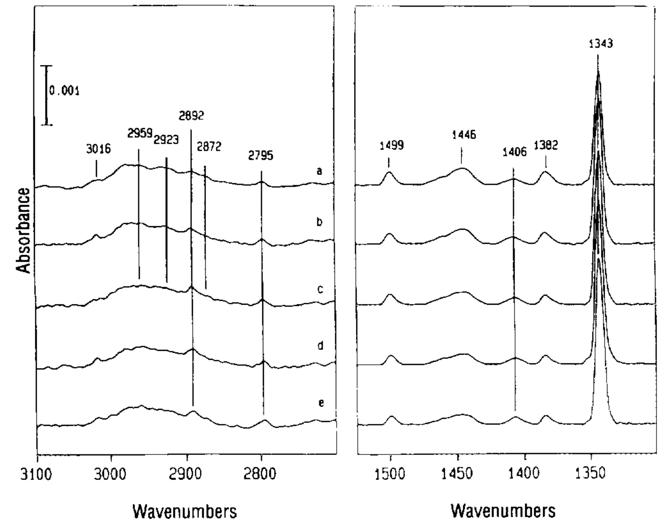

FIG. 6. FT-IR spectra recorded of adsorbed C_2H_5Cl on Pt/SiO_2 as a function of temperature: (a) 200 K, (b) 226 K, (c) 247 K, (d) 256 K, (e) 286 K.

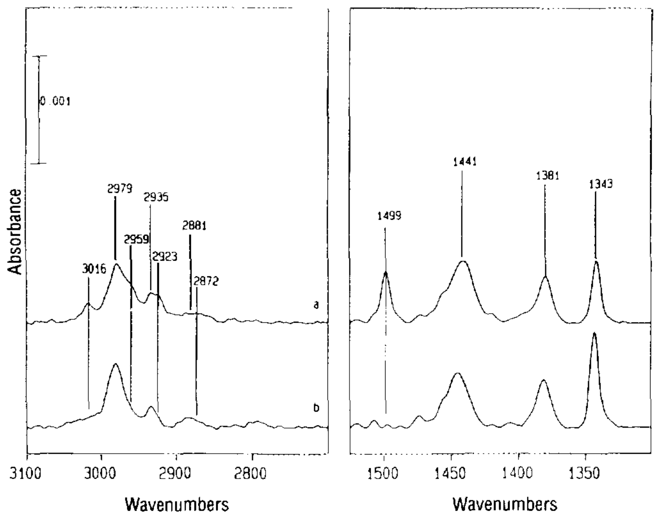

FIG. 7. FT-IR spectra recorded of C_2H_5Cl on Pt/SiO_2 at 200 K after evacuation for 15 minutes; (a) before and (b) after addition of H_2. Bands due to C_2H_5 (2959, 2923, and 2872 cm^{-1}) and π-bonded C_2H_4 (3016 and 1499 cm^{-1}) disappear from the spectrum upon addition of H_2 whereas bands due to C_2H_5Cl (2979, 2935, 2881, 1441, and 1381 cm^{-1}) and C_2H_3 (1343 cm^{-1}) remain.

bands do not decrease in intensity upon the addition of hydrogen.

4. *Reaction of C_2H_5Cl at 473 K on Pt/Al_2O_3 and Pt/SiO_2*

The reaction of C_2H_5Cl on Pt/SiO_2 and Pt/Al_2O_3 was monitored in both the presence and the absence of H_2 at 473 K with infrared spectroscopy and mass spectrometry. Figure 8a shows the infrared spectrum of 10.0 Torr C_2H_5Cl on Pt/Al_2O_3 immediately after introduction to the sample cell. The catalyst was then heated to 473 K and the progress of the decomposition reaction was monitored using IR spectroscopy. The difference spectrum recorded after heating to 473 K for 15 min is shown in Fig. 8b. The difference spectrum shows the loss (negative features) of C_2H_5Cl absorption bands due to depletion from reaction and the growth (positive features) of product bands. There is a loss of about 17% of C_2H_5Cl as measured by a decrease in the integrated area of the parent absorption bands after 15 min. Because of overlapping reactant and product absorption bands, the bands between 900 and 1300 cm^{-1} were used to determine the percentage of C_2H_5Cl loss. The most obvious feature in the difference spectra is the rotational structure centered near 2800 cm^{-1} due to gas-phase HCl. The identity of the hydrocarbon products that form is not clear from the IR data because of overlapping bands in the 2900–3100 cm^{-1} region for C_2H_5Cl, C_2H_6, C_2H_4, and CH_4. Also shown in Fig. 8 is the difference spectrum after reaction of ethyl chloride and an equal amount of hydrogen (Fig. 8c). There is a loss of approximately 35% in the integrated area of the parent ethyl chloride absorption bands after 15 min of reaction. The reaction rate for C_2H_5Cl decomposition on Pt/Al_2O_3 is enhanced in the presence of H_2. C_2H_5Cl reaction on a Pt/SiO_2 catalyst gave similar results.

To identify hydrocarbon product formation, ethyl chloride reaction at 473 K was monitored with mass spectrometry as a function of reaction time. The mass spectral data for reaction of C_2H_5Cl on Pt/Al_2O_3 in the absence and presence of hydrogen are shown in Figs. 9 and 10. A decrease in the amount of C_2H_5Cl ($m/e = 64$) is evident as the reaction proceeds. The decrease of C_2H_5Cl is concomitant with the growth of HCl ($m/e = 36$) as previously determined by infrared spectroscopy. The mass spectral data also show evidence for the production of ethylene, ethane, and some methane. For ethylene, the $C_2H_3^+$ ion ($m/e = 27$) was used to measure the amount of ethylene produced. To determine the amount of ethylene formed, the $C_2H_3^+$ ion signal was corrected for fragmentation of C_2H_5Cl and C_2H_6 (23). The mass spectral data show that there is a difference in the amount of C_2H_5Cl that reacts and the product distribution when hydrogen is present. With hydrogen, C_2H_5Cl reacts to a greater extent and ethane production is enhanced relative to ethylene.

5. *Reaction of C_2H_5Cl at 473 K on Al_2O_3 and SiO_2*

Although C_2H_5Cl does not react with either silica or alumina at low temperatures (near 200 K), at 473 K ethyl

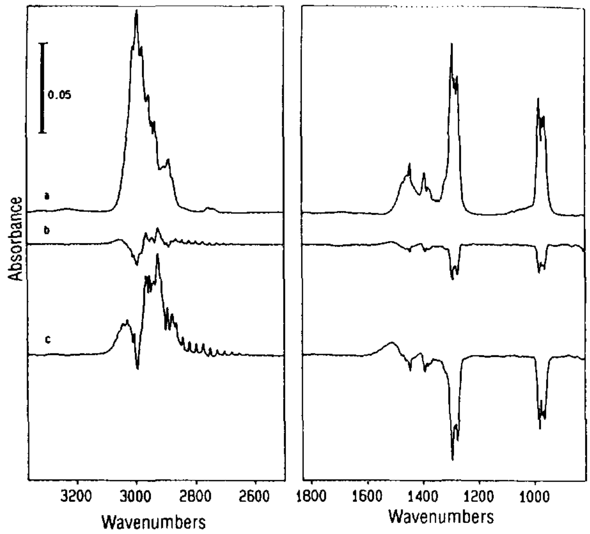

FIG. 8. (a) Infrared spectra recorded of gas-phase C_2H_5Cl (10 Torr) in the presence of Pt/Al_2O_3 before heating to 473 K. (b) Difference spectrum recorded after heating to 473 K for 15 min showing the loss of gas-phase C_2H_5Cl due to reaction. (c) Difference spectrum recorded after heating C_2H_5Cl in the presence of an equal amount of hydrogen to 473 K for 15 min. The data show that the decomposition of C_2H_5Cl is enhanced in the presence of H_2.

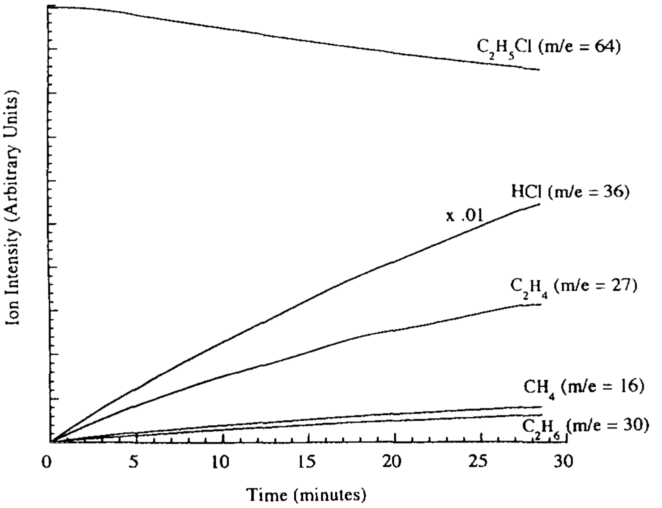

FIG. 9. Mass spectral data recorded as a function of reaction time for C_2H_5Cl (10 Torr) in the presence of Pt/Al_2O_3 at 473 K. A loss of C_2H_5Cl (*m/e* = 64), and growth of C_2H_4 (*m/e* = 27), HCl (*m/e* = 36), C_2H_6 (*m/e* = 30), and CH_4 (*m/e* = 16) is evident over time.

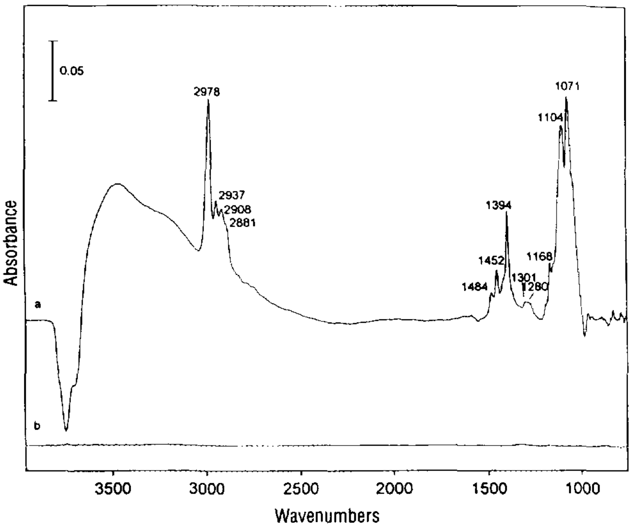

FIG. 11. Infrared spectra recorded after reaction of 10 Torr of C_2H_5Cl with (a) Al_2O_3 and (b) SiO_2 at 473 K. The spectra were recorded after evacuation of gas-phase reactants and products. Al_2O_3 does react with C_2H_5Cl to form surface ethoxy groups. Under similar conditions, no reaction is evident on the silica surface.

chloride does react with Al_2O_3. Ten Torr of C_2H_5Cl was introduced into the infrared cell containing alumina; the alumina sample was then heated to 473 K for 15 min. The infrared spectrum recorded after evacuation of gaseous C_2H_5Cl is shown in Fig. 11a. The spectrum shows intense absorption bands with frequencies of 2978, 2937, 2908, 2881, 1484, 1452, 1394, 1301, 1280, 1168, 1104, and 1071 cm^{-1}. These bands do not decrease in intensity as a function of evacuation time. The spectrum shown in Fig. 11 is nearly identical to the IR spectrum that results after reaction of ethanol with Al_2O_3 to give ethoxy groups (24, 25). The infrared spectrum of ethoxy groups is assigned in Table 2 using the assignment of Street and Gellman (26). The negative feature in the hydroxyl group region shows there is a loss of hydroxyl groups on the alumina surface upon reaction with C_2H_5Cl suggesting that surface hydroxyl groups play a role in the reaction. There is no reaction of C_2H_5Cl with silica at temperatures below 573 K (Fig. 11b).

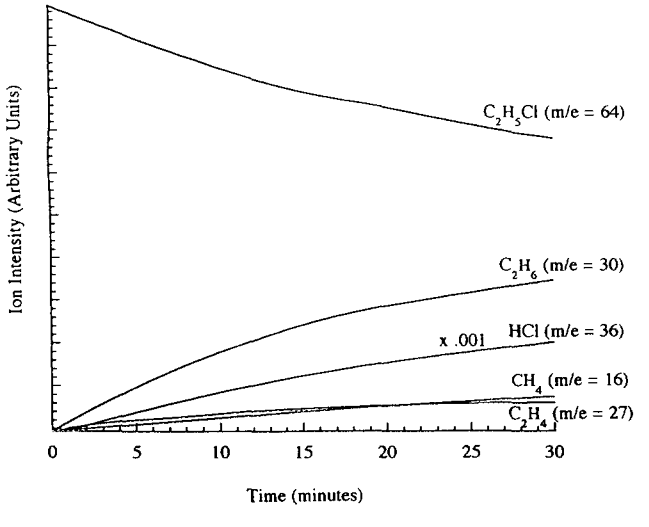

FIG. 10. Mass spectral data recorded as a function of reaction time for C_2H_5Cl (10 Torr) and H_2 (10 Torr) in the presence of Pt/Al_2O_3 at 473 K. A loss of C_2H_5Cl (*m/e* = 64) and growth of C_2H_6 (*m/e* = 30), HCl (*m/e* = 36), C_2H_4 (*m/e* = 27), and CH_4 (*m/e* = 16) is evident over time.

DISCUSSION

Reaction products detected by infrared spectroscopy and mass spectrometry for low- and high-temperature reaction of C_2H_5Cl with oxide-supported Pt catalysts are summarized in the schematic shown in Fig. 12. At low temperatures, C_2H_5Cl can desorb from the Pt particles or dechlorinate to give adsorbed π-bonded ethylene or ethyl. Ethyl groups dehydrogenate to give ethylidyne between approximately 200 and 285 K. π-Bonded ethylene slowly desorbs from the surface near 295 K. Both π-bonded ethylene and ethyl readily hydrogenate upon addition of hydrogen. At high temperatures, a limited amount of C_2H_5Cl decomposes to give predominately gas-phase C_2H_4 and HCl. In the presence of hydrogen, C_2H_5Cl decomposes to a greater extent to give predominantly gas-phase C_2H_6 and HCl. Some methane is formed as well at these higher temperatures. Possible reaction mechanisms for the low- and high-temperature reaction of C_2H_5Cl with oxide-supported Pt catalysts are discussed in more detail below.

TABLE 2
Vibrational Assignment of Ethoxide, OCH_2CH_3

Mode description[a]	C_2H_5OH (liquid)	C_2H_5O–Cu(111)[b]	C_2H_5O–Al[c]
CH_3 *a*-stretch	2975	2955	2978
CH_3 *s*-stretch	2928	n.o.	2937
CH_2 *s*-stretch	2894	2857	2908, 2881
CH_3 *a*-deform	1445	1444	1452, 1484
CH_3 *s*-deform	1380	1380	1394
CH_2 scissor	1330	1354	1301
CH_2 twist	1274	n.o.	1280
CH_3 rock	1152	n.o.	1168
Combination mode	n.o.	1093	1104
CCO a-stretch	1049	1048	1071

[a] Ref. (27).
[b] Ref. (26).
[c] This work.

1. *Low-Temperature Reaction of C_2H_5Cl with Pt/SiO_2 and Pt/Al_2O_3: Mechanisms of Formation of Adsorbed C_2H_x Fragments*

The IR data show the presence of several C_2 fragments after adsorption of C_2H_5Cl on Pt/SiO_2 and Pt/Al_2O_3 from approximately 200–285 K. The growth behavior of these fragments are different and suggest that they arise from different reaction mechanisms. The following competing reactions would account for the experimental data:

$$C_2H_5Cl\,(a) \rightarrow C_2H_5Cl\,(g) \qquad \text{Desorption} \qquad [4]$$

$$C_2H_5Cl\,(a) \rightarrow \pi\text{-}C_2H_4\,(a) + HCl\,(a) \qquad \alpha,\beta\text{-Elimination} \qquad [5]$$

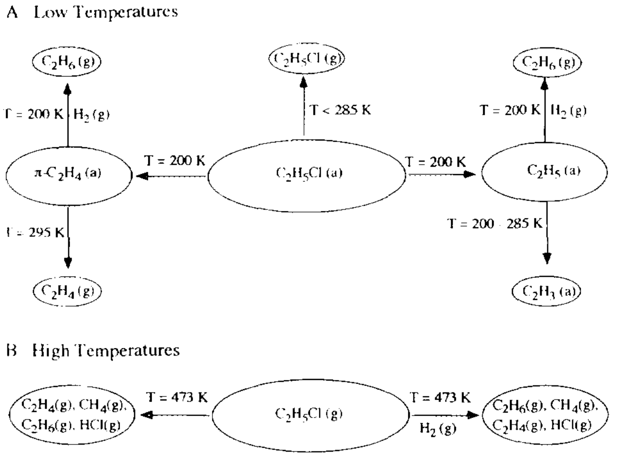

FIG. 12. Schematic summarizing products detected with infrared spectroscopy and mass spectrometry from reaction of C_2H_5Cl on oxide-supported Pt catalysts at (A) low and (B) high temperatures.

$$C_2H_5Cl\,(a) \rightarrow C_2H_5\,(a) + Cl\,(a) \qquad \text{C-Cl Bond dissociation.} \qquad [6]$$

First, there is loss of adsorbed C_2H_5Cl due to desorption into the gas phase (Eq. [4]). The desorption of C_2H_5Cl uncovers sites on the Pt surface for further reaction. C_2H_5Cl can then react at low temperatures to yield dechlorinated C_2 species on the surface. It is clear from the differences in the growth behavior of π-bonded ethylene and ethylidyne that these two species form as a result of two different reaction mechanisms. One possible reaction pathway for the formation of π-bonded ethylene is through α, β-elimination of HCl (Eq. [5]). The fate of the HCl produced in the reaction is unclear. HCl can either dissociate on the surface to form adsorbed hydrogen and chlorine atoms or it can desorb into the gas phase. A second competing reaction pathway that can explain the growth behavior of ethylidyne is one that initially involves C–Cl bond dissociation to form adsorbed ethyl groups (Eq. [6]) followed by dehydrogenation of ethyl to ethylidyne. The two reaction pathways, C–Cl bond dissociation and HCl elimination, may have different site requirements on the Pt catalyst.

Several studies of ethyl halides on single-crystal Pt surfaces have also shown the presence of adsorbed ethyl groups. White and co-workers examined ethyl groups on the surface of Pt (111) formed from the photodissociation of adsorbed ethyl chloride at 100 K (5, 6). Upon heating to 230 K ethyl groups dehydrogenate to form di-σ-bonded ethylene. Further heating to 320 K resulted in conversion of ethylene to ethylidyne. They concluded that di-σ-bonded ethylene was the stable intermediate to dehydrogenation of ethyl to ethylidyne. Zaera and co-workers have used X-ray photoelectron, infrared, and temperature-programmed desorption spectroscopy to study the thermal decomposition of ethyl iodide on Pt(111) between 100 and 300 K (28, 29). They also observed the formation of ethylene and ethyl on the surface between 170 and 270 K. They propose that the stability of ethyl on the surface is due to the interconversion of C_2H_4 and C_2H_5 through fast hydrogen transfer. The supporting evidence for this was H–D scrambling when partially deuterated ethyl iodide and coadsorbed deuterium reacted to form ethane and ethylene on the surface.

On the oxide-supported catalyst, the formation of ethylidyne appears to be coupled to the disappearance of adsorbed ethyl groups suggesting that ethyl groups dehydrogenate to ethylidyne. The data indicate that ethylidyne formation does not occur through the conversion of π-bonded ethylene, in accord with earlier investigations of ethylene adsorption on oxide-supported Pt (14, 17). Although it appears that ethyl groups dehydrogenate to form ethylidyne, it is unclear from the data what the mechanism is for this reaction, i.e, whether C_2H_5 dehydrogenates through a di-σ-bonded C_2H_4 intermediate or some other intermediate. One plausible explanation for the fact that we find no evidence for di-σ-bonded C_2H_4 is that it may rapidly convert to ethylidyne at temperatures between 200 and 285 K at a rate that may be too fast to observe on the time scale of the infrared measurements. Mohsin *et al.* observe the complete conversion of di-σ-bonded ethylene on Pt/Al_2O_3 to ethylidyne at a temperature as low as 180 K (17).

2. *Hydrogenation of C_2H_x Fragments at Low Temperature*

The infrared data show that absorptions bands due to adsorbed ethyl and π-bonded ethylene disappear upon addition of hydrogen to presumably form gas-phase ethane whereas absorptions bands due to ethylidyne do not decrease upon addition of hydrogen. These data indicate that C_2H_5 and C_2H_4 are more easily hydrogenated than C_2H_3. The relative ease of hydrogenation of these C_2 fragments is in accord with other studies of ethylene hydrogenation. Previous studies have shown that the π-bonded and di-σ bonded forms of ethylene can be hydrogenated much faster than ethylidyne (17). The reactivity of the C_2 hydrocarbon fragments with hydrogen provide additional support of the assignments made for these species.

3. *Reaction Mechanisms for High-Temperature Reaction of C_2H_5Cl with Pt/Al_2O_3, Pt/SiO_2, Al_2O_3, and SiO_2*

The decomposition of ethyl chloride at 473 K produces gas-phase products that have been identified by mass spectrometry. Reaction with and without hydrogen shows differences in the amount of C_2H_5Cl converted as well as in the product distribution.

Both hydrogenation and dehydrogenation occur for C_2 fragments adsorbed on metal surfaces and many studies have investigated these reactions on Pt surfaces. For ethylene in the presence of excess hydrogen, the rate of production of ethylidyne is reduced and the hydrogenation of ethylene and ethyl to ethane is enhanced (30, 31). Yagasaki and Masel have done coadsorption studies of ethylene and hydrogen on a (2 × 1) Pt(111) surface (30). They found decreased formation of di-σ-bonded C_2H_4 compared to π-bonded C_2H_4 when ethylene was adsorbed onto a hydrogen-saturated surface, which ultimately inhibited the formation of ethylidyne. Similar results were found by Zaera when ethyl iodide and hydrogen were coadsorbed in Pt(111) (31).

Central to the practicality of Pt/SiO_2 and Pt/Al_2O_3 as decomposition catalysts is the regeneration of active metal sites. It seems from the single-crystal data that if ethylene can be hydrogenated before it is converted to ethylidyne, the Pt surface can remain active. As shown here, hydrogen plays a critical role in the reaction of ethyl chloride on the oxide-supported Pt catalyst. Hydrogen reacts with adsorbed dechlorinated C_2 species to form gas-phase ethane and inhibits the formation of ethylidyne. Hydrogen also plays a role in the removal of adsorbed chlorine atoms to form gaseous hydrogen chloride.

An earlier study by Campbell and Kemball examined carbon–halogen bond breaking of ethyl chloride in the presence of hydrogen on evaporated Pd, Pt, Ni, Fe, W, and Rh films using mass spectrometry (32). The following thermodynamically feasible reactions were considered in their studies:

$$C_2H_5Cl\,(g) \rightarrow C_2H_4\,(g) + HCl\,(g) \qquad [7]$$

$$C_2H_5Cl\,(g) + H_2\,(g) \rightarrow C_2H_6\,(g) + HCl\,(g) \qquad [8]$$

$$C_2H_5Cl\,(g) + 2\,H_2\,(g) \rightarrow 2\,CH_4\,(g) + HCl\,(g). \qquad [9]$$

The reaction shown in Eq. [8] was shown to be the predominant reaction on evaporated Pt films. The results presented here are consistent with this earlier study, although there is evidence for all three reactions shown in Eqs. [7–9]. However, the reaction shown in Eq. [8] dominates in the presence of hydrogen.

It should be noted that the low- and high-temperature results presented in this study correlate very well with each other suggesting that some of the intermediates detected at low temperatures may form during reaction at the higher temperatures. At low and high temperatures, in the absence of hydrogen, dehydrogenation results in the formation of ethylidyne on the surface and ethylene in the gas phase. At low temperatures, upon addition of hydrogen, adsorbed C_2 fragments hydrogenate to ethane and at high temperatures, ethane is the predominant reaction product.

Finally, the role of the support in catalysis is always an important consideration. In contrast to alumina, silica does not react with C_2H_5Cl (see Fig. 11) at temperatures below 573 K. However, the infrared data clearly demonstrate that alumina reacts with ethyl chloride to give surface-bound ethoxy groups. Loss of surface hydroxyl groups after reaction with C_2H_5Cl suggest that they participate in the reaction. The infrared results are consistent with the following reaction where surface OH groups are consumed upon reaction:

$$C_2H_5Cl\,(g) + AlOH\,(s) \xrightarrow{473\text{ K}} AlOCH_2CH_3\,(s) + HCl\,(g). \qquad [10]$$

There is some precedence for this type of reaction. Beebe *et al.* investigated the reaction of methyl chloride with alumina (33). Surface methoxy and gaseous hydrogen chloride form at temperatures above 300 K in a reaction mechanism similar to that shown in Eq. [10]. The exact role that ethoxy groups may play in further reaction of C_2H_5Cl with Pt/Al_2O_3 is not entirely clear from the data. The decomposition of chlorides to form alkoxides on Pt/Al_2O_3 may present a new pathway for the formation of oxygenates, such as alcohols from chlorides. However, further study is required to determine the feasibility of this type of reaction.

ACKNOWLEDGMENTS

Acknowledgment is made to the donors of the Petroleum Research Fund, administered by the American Chemical Society, for partial support of this research. The authors also gratefully acknowledge the National Science Foundation (Grant CHE-9300808) for support of this research.

REFERENCES

1. Hoffman, M. R., Martin, S. T., Choi, W., and Bahnemann, D. W., *Chem. Rev.* **95,** 69 (1995), and references therein.
2. Windawi, H., and Wyatt M., *Platinum Metal Rev.* **37,** 186 (1993).
3. Muller, H., Deller, K., Despeyroux, B., Peldszuc, E., Kammerhofer, P., Kuhn, W., Spielmannleither, R., and Stoger, M., *Catal. Today* **17,** 383 (1993).
4. McGee, K. C., Driessen, M. D., and Grassian, V. H., *J. Catal.* submitted.
5. Lloyd, K. G., Roop, B., Campion, A., and White, J. M., *Surf. Sci.* **214,** 227 (1989).
6. Lloyd, K. G., Campion, A., and White, J. M., *Catal. Lett.* **2,** 105 (1989).
7. McGee, K. C., Capitano, A. T., and Grassian, V. H., *Langmuir* **10,** 632 (1994).
8. Yates, Jr., J. T., Duncan, T. M., and Vaughan, R. W., *J. Chem. Phys.* **71,** 3908 (1979).
9. Beebe, Jr., T. P., Gelin, P., and Yates, Jr., J. T., *Surf. Sci.* **148,** 526 (1984).
10. Beebe, Jr., T. P., Ph. D. dissertation, University of Pittsburgh, 1987.
11. Sheppard, N., and Nguyen, T. T:, *in* "Advances in Infrared and Ramen Spectroscopy" (R. Clark and R. E. Hester, Eds.), Vol. 5. Heydon, London, 1978.
12. Bandy, B. J., Chesters, M. A., James, D. I., McDougall, G. S., Pemble, M. E., and Sheppard, N., *Philos. Trans. Soc. London, Ser. A* **318,** 141 (1986).
13. Prentice, J. D., Lesiunas, A., and Sheppard, N., *J. Chem. Soc. Chem. Commun.*, 76 (1976).
14. de la Cruz, C., and Sheppard, N., *J. Chem. Soc. Chem. Commun.*, 1854 (1987).
15. de la Cruz, C., and Sheppard, N., *J. Mol. Struct.* **247,** 25 (1991).
16. Beebe, Jr., T. P., and Yates, Jr., J. T., *J. Phys. Chem.* **91,** 254 (1987).
17. Mohsin, S. B., Trenary, M., and Robota, H. J., *J. Phys. Chem.* **92,** 5229 (1988).
18. Primet, J., and Sheppard, N., *J. Catal.* **41,** 258 (1976).
19. Hair, M. L., "Infrared Spectroscopy in Surface Chemistry," Dekker, New York, 1967.
20. Pimentel, G. C., and McClellan, A. L., "The Hydrogen Bond." Freeman, San Francisco, 1960.
21. Shimanouchi, T., "Tables of Molecular Vibrational Frequencies," Vol. 1. National Standard Reference Data Series, NBS (U.S.), 1962.
22. Greenler, R. G., Snider, D. R., Witt, D., and Sorbello, R. S., *Surf. Sci.* **118,** 425 (1982).
23. Mass spectral fragmentation pattern of C_2H_5Cl gave a relative m/e ratio for 64:27 of 1:1.54. The fragmentation pattern of C_2H_6 at an ionization energy of 70 eV was taken from Stenhagen, E., Abrahamsson, S., and McLafferty, F. W., "Atlas of Mass Spectral Data," Vol. 1. Wiley, New York, 1969.
24. Greenler, R. G., *J. Chem. Phys.* **37,** 2094 (1962).
25. DeCanio, E.C., Bruno, J. W., Nero, V. P., and Edwards, J. C., *J. Catal.* **140,** 84 (1993).
26. Street, S. C., and Gellman, A.J., *J. Chem. Phys.*, in press.
27. Perchard, J.-P., and Josien, M.-L., *J. Chim. Phys.-Chim. Biol.* **65,** 1834, 1856 (1969).
28. Hoffman, H., Griffiths, P. R., and Zaera, F., *Surf. Sci.* **262,** 141 (1992).
29. Zaera, F., *Surf. Sci.* **219,** 453 (1989).
30. Yagasaki, E., and Masel, R. I., *Surf. Sci.* **226,** 51 (1990).
31. Zaera, F., *J. Phys. Chem.* **94,** 8350 (1990).
32. Campbell, J. S., and Kemball, C., *Trans. Faraday Soc.* **57,** 809 (1961).
33. Beebe, Jr., T. P., Crowell, J.E., and Yates, Jr., J. T., *J. Phys. Chem.* **92,** 1296 (1988).